**DOR: 20.1001.1.27170314.2022.11.4.3.5**

Research Paper

# Comparison of the Behavior of Martensitic and Ferrite Samples on Acoustic Emission Parameters

**Ramin Khamedi[1,2], Mehdi Khosravi[2*]**
[1]Department of Mechanical Engineering, Khazar University, Baku, Azerbaijan
[2]Department of Mechanical Engineering, Zanjan University, Zanjan, Iran
[*]Email of Corresponding Author: mehdi.khosravi@znu.ac.ir
*Received: November 15, 2022; Accepted: December 30, 2022*

**Abstract**
This study aimed to compared mechanical properties and failure mechanisms in ferrite and martensite samples, using Acoustic Emission (AE) Non-Destructive Testing (NDT). The purpose of this study is to identify the phases of ferrite and martensite by analyzing the parameters of AE. Tensile testing was performed on the samples and AE signals were recorded. The Sentry Function (SF) and Fast Fourier Transform (FFT) were used to analyze signals. The results of the martensite sample show that the SF is almost constant at the beginning. This indicates a relative balance between the AE energy and the strain energy. Then the SF took a downward state, which demonstrates a greater ratio of acoustic energy to strain energy. Frequency distribution, one of the best parameters to identify the failure mechanisms in materials for the ferrite sample, is significantly in the range of 175 kHz, while for the martensite sample, this range is between 520 and 700 kHz.

**Keywords**
Martensitic, Acoustic Emission, Fast Fourier Transform, Sentry Function

## 1. Introduction

Dual-Phase (DP) steels are composed of two phases: soft ferrite and hard martensite. The ferrite phase has a bcc structure that can hold a small percentage of carbon [1-2]. In rapid cooling, there is not enough time for the movement of carbon atoms from the crystal structure of austenite, and they are locked in the fcc structure, and martensite is formed due to the complex cutting of the fcc structure, which is the result of local stress concentration. The diagram in Figure 1 [3] shows the effect of cooling speed on the microstructure.

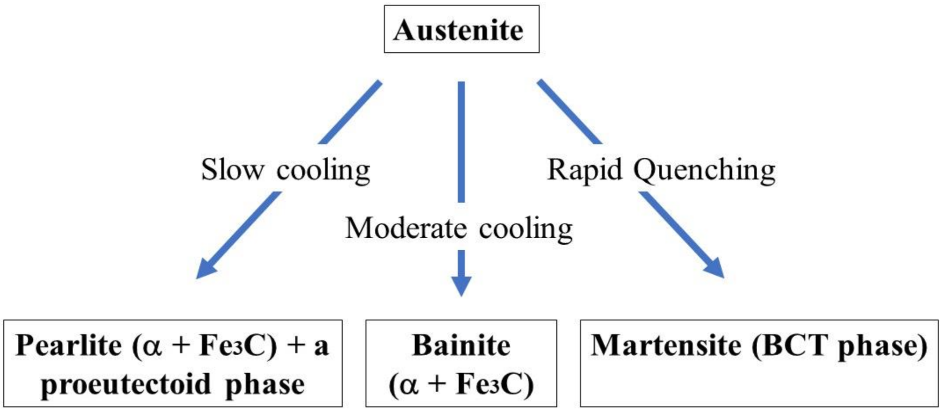


Figure 1. Effect of cooling rate on microstructure [3]

Lath martensite structure is the most common that occurs in low and medium-carbon steels (Figure 2). Lath Martensite grows as a parallel cluster of laths that are about 0.1 to 0.5 microns thick. A light microscope illustrates the clusters of laths however; it is not possible to see individual laths with this light [4].

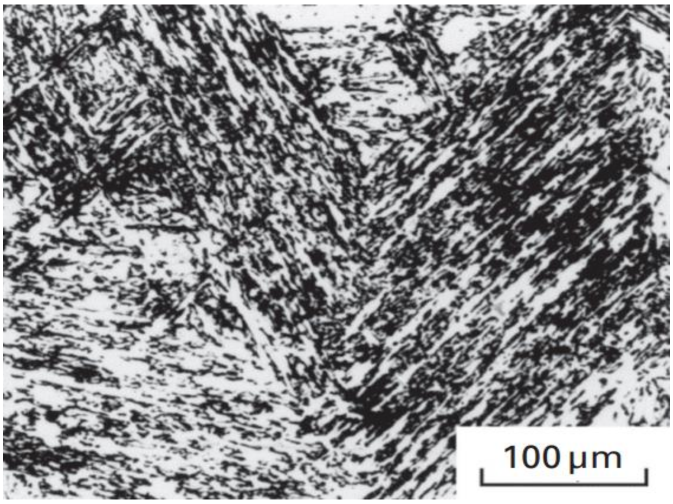


Figure 2. Lath martensite [4]

According to the definition of the American Society for Testing and Materials (ASTM), Acoustic Emission (AE) refers to a class of dynamic phenomena in which transient elastic waves or in other words, sound waves due to the rapid release of strain energy in local sources and permanent deformation (redistribution of the stress field) ) occur in materials under stress [5]. These waves are spread in a very wide frequency range and after passing through the environment, they stimulate certain sensors and these sensors give voltage output. For this amplified and filtered voltage, statistical analysis algorithms are applied. AE is a powerful tool to investigate and study deformation and failure in materials. AE signals were analyzed with different methods, including Wavelet Packet Transform (WPT), Fast Fourier Transform (FFT), and Clustering methods.

Many researchers have conducted extensive research to investigate the failure mechanisms of ferrite and martensite phases using AE [6-14]. Speich et al. [15] have studied martensite formation in a Fe-28 using AE. Their results show that about 15 martensitic plates are involved in each AE and more detailed studies of the transformation kinetics, can be made with this technique because AE gives an almost plate-by-plate record of the martensitic transformation. Planes et al. [16] did research on AE originating during martensitic transformations. Their results show that analyzing AE within an appropriate framework is a very useful technique, which provides quantitative dynamical information complementary to that obtained from more standard techniques. The probability density function of amplitudes, energies, and durations of the detected acoustic signals follows power-law distributions related to avalanche criticality. Examples of non-magnetic and magnetic shape-memory alloys under selected external conditions indicate this.

This research is a continuation of the paper [17], in which ferrite samples were tested using AE. The purpose of this research is to compare the results obtained from the tensile test on ferrite and martensite samples using AE signals. For this aim, iron with a very low carbon percentage and C40 steel was used to make ferrite and martensite samples. To analyze the AE signals, apart from the FFT method, which is used to identify the frequency parameter, the Sentry Function (SF) method has been used, which is a new method.

## 2. Experimental procedure

To perform the tensile test ferrite and almost 100% martensite samples were made. Table 1 shows the chemical composition of the manufactured samples. In this research, ferrite and martensite samples were made according to the ASTM E08 standard with a width of 12 mm, a thickness of 2 mm, and a length of 35 mm. The samples with low impurity of Sulphur and Phosphorus were chosen to minimize the effects of coarse inclusions [18].

Table 1. Chemical composition of the metal used (weight percentage)

| | C | Mn | Si | Al | Nb | P | S | Cu | Fe |
|---|---|---|---|---|---|---|---|---|---|
| Martensit | 0.43 | ---- | ---- | ---- | ---- | 0.018 | 0.009 | ---- | Bal |
| Ferrite | 0.003 | 0.31 | 0.03 | ---- | ---- | 0.025 | 0.04 | 0.032 | Bal |

C40 steel was used to make a full martensitic sample and check its effect on AE signals. This steel was placed at a temperature of 920 ° C and after one hour, it was rapidly cooled in a mixture of ice and saltwater at a temperature of -8° C. The obtained sample had a lath martensite structure with a high percentage of martensite phase .

The cross-section of the samples was polished for metallography and checking the size of the ferrite grains, which were manufactured by Remet. After finishing the polishing operation, the cross-sections of the samples were etched in a 2% nital solution. The tensile test was done with Instron 8032 device with 250 kN capacity and a speed of 0.05 mm/sec. The tests were performed with the PAC-PCI-DSP4 ultrasonic transmission system with the capacity of using four sensors. In AE Win software, the threshold parameter was set to 30dB to remove environmental noises.

## 3. Sentry Function

The SF is the logarithm of the ratio of mechanical energy to acoustic energy .The function represents the continuous balance between the stored strain energy and the acoustic energy released due to damage. This function is usually discrete and is expressed by a combination of the four functions.

When significant internal refraction occurs within the material, is released a significant amount of AE which produces high-energy acoustic signals, resulting in a sudden drop in the function .The function can be used to advance damage within the material by using mechanical and acoustic information. In addition, because the above function contains the entire history of damage growth, it can be used as a criterion to determine the remaining life of the material. In this case, the integral of the function can be used to achieve this goal.

## 4. Results of ferrite and martensite samples

Figure 3 shows the metallographic samples of ferrite and martensite produced by heat treatment of C40 steel.

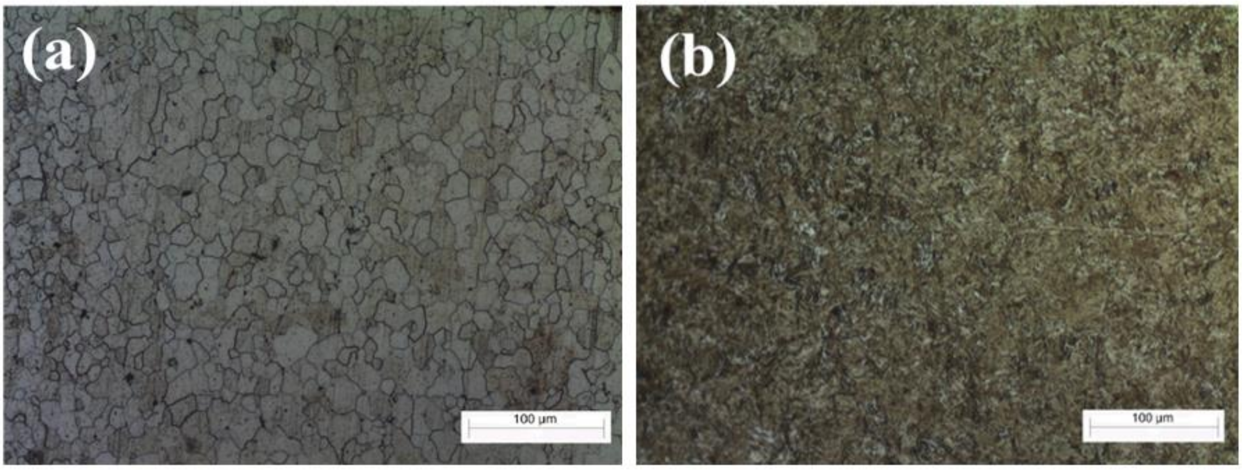


Figure 3. Optical metallographic images of typical low carbon ferritic steels: Ferrite (a), and Martensite C40 (b)

The purpose of the tests performed on ferrite and martensite samples is to investigate the behavior of the ferrite and martensite phases independently of the AE results. For this purpose, the tensile standard sample of C40 steel was placed at a temperature of 920 ° C and after one hour, it was rapidly cooled in a mixture of ice and saltwater at a temperature of -8° C. The sample had a lath martensite structure. Figure 4 shows the results obtained from martensite samples. The results of these tests are shown in Table 2.

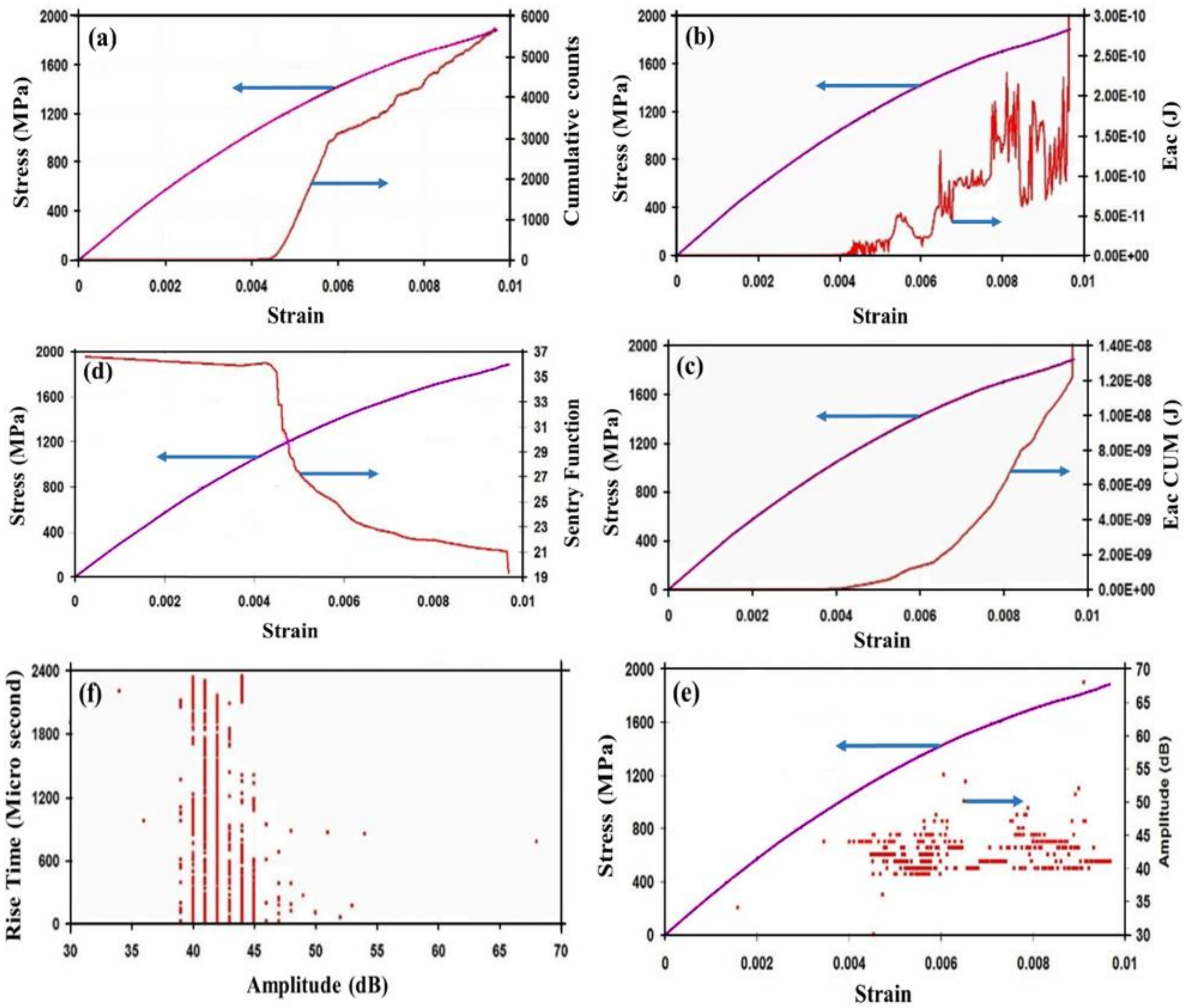


Figure 4. Stress-strain diagram in the Martensitic and Cumulative Count (a), Acoustic Energy (b), Cumulative Acoustic Energy (c), Sentry Function (d), Amplitude (e), and Rise Time with Amplitude (f)

Table 2. Mechanical properties and acoustic results of ferrite and martensite

| Full Annealing temperature°C (Samples codes) | Ferrite grain size (μm) | YS | UTS | $\varepsilon_t$ (%) | n | Max Eac (J) | Max Risetime (μSec) | Average Amp. (dB) | Average Risetime (μSec) | Count Cum |
|---|---|---|---|---|---|---|---|---|---|---|
| Ferrite (F) | 9.6 | 286 | 587 | 29.5 | 0.26 | $2.5\times10^{-9}$ | 680 | 32.19 | 26.64 | $4.7\times10^{+4}$ |
| 920 (C40 Martensite) | ---- | 1650 | 2100 | 1 | 0.56 | $2.3\times10^{-10}$ | 2345 | 41.66 | 173.43 | 5694 |

According to Figure 4 and Table 2, the mechanical behavior of the ferrite sample is almost consistent with the Hall-Petch equation. The amount of n (work hardening exponent) is approximately equal to the amount of strain at the beginning of non-uniform deformation or the maximum force applied during the tensile test [19]. The average amplitude in the martensite sample is higher than in the ferrite sample, which confirms the work of previous researchers [20-21], and the maximum rise time in the martensite sample is higher than in the ferrite sample.

Another important point is the amount of AE energy released in the tensile test. In Figure 4 (d), it is clear that the SF is almost constant before the strain of 0.004, indicating a relative balance between the AE energy and the strain energy. After this strain, the SF takes a downward state and indicates a more ratio of acoustic energy to strain energy, and this shows the existence of a significant amount of AE energy at the strain of 0.0045 until failure. It means that significant failure in the martensitic sample has started from this strain. This can also be seen in Figure 4 (c), which corresponds to the cumulative AE energy. These results show a significant difference with the ferrite sample that function has a completely ascending state after yielding.

Figure 5 shows the distribution of the AE amplitude in the tensile test of the martensite sample. Figure 5 shows, the maximum density of the domains is in the range of 40-45 dB. Figure 4 (e) indicates this issue, while the amplitude distribution in the ferrite sample is approximately between 30-40 dB, which is related to the deformation of the ferrite phase. Figure 4 (f) shows the rise time distribution in the martensite sample up to about 2400 microseconds while the maximum rise time in the ferrite sample is about 700-800 microseconds. This issue shows the difference related to maximum rise time and amplitude distribution for the martensite and ferrite samples.

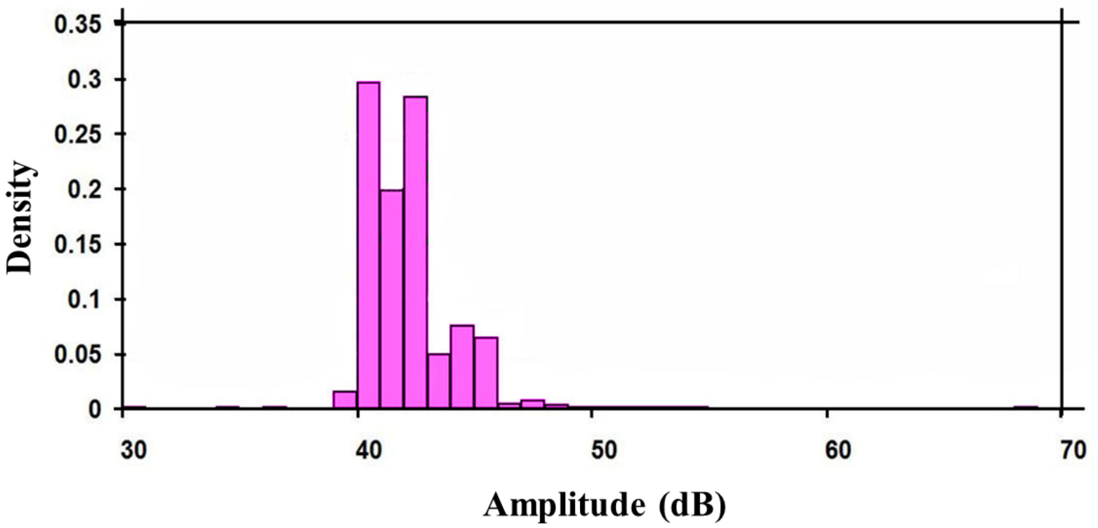


Figure 5. Amplitude distribution in the tensile test of a martensite sample

The FFT method was used to take the dominant frequency. Figures 6 and 7 show the dominant frequency distribution in the tensile test of ferrite and martensite samples. As can be seen, the frequency distribution for the ferrite sample in the range of 175 kHz has a higher density, which agrees with previous researchers' results [20-21]. Nevertheless, the frequency distribution for the martensite sample is between 520-700 kHz, which is different from the dominant frequency in the ferrite sample. This case is another characteristic that can be used for analysis and to distinguish failure mechanisms from each other [22-23].

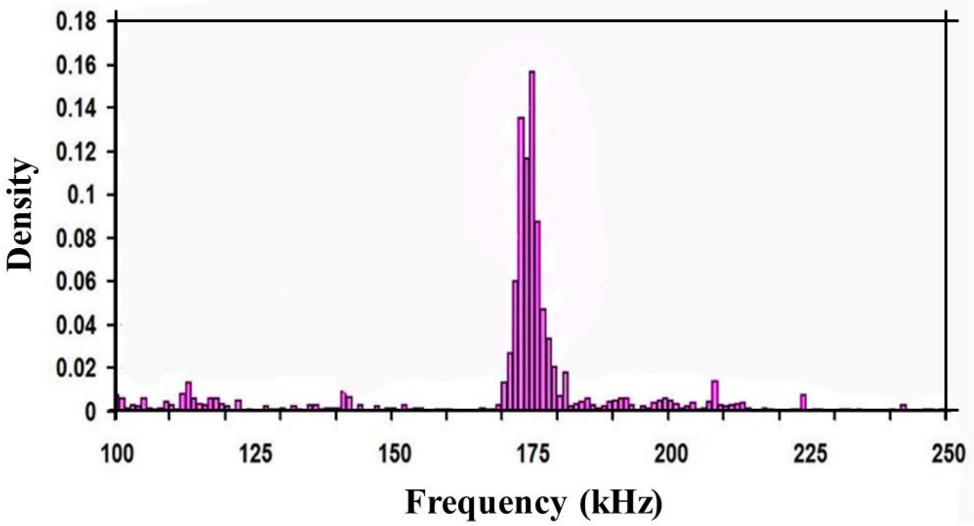


Figure 6. Dominant frequency distribution in the tensile test of ferrite sample

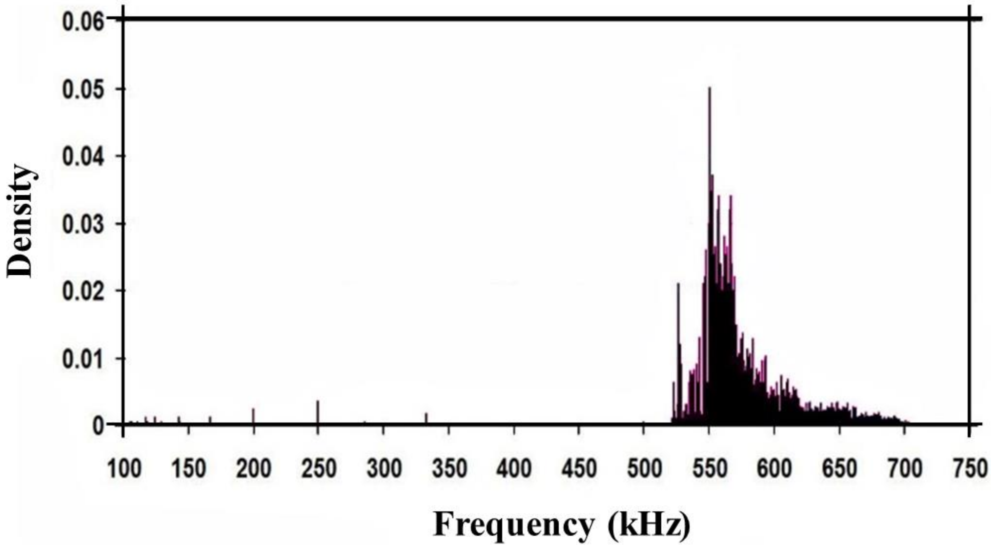


Figure 7. Dominant frequency distribution in the tensile test of a martensite sample

By using the results obtained from the analysis of AE signals as well as their analysis with FFT and SF methods, it is possible to achieve desirable results of the failure mechanisms in the ferrite and martensite phases separately. These results can be used to identify failure mechanisms in dual-phase steels with different volume fraction percentages.

## 5. Conclusion

In this research, the behavior of the ferrite and martensite phases was investigated independently on AE results. A sample of C40 steel was used to make the martensite phase. For this purpose, this sample was placed at a temperature of 920 ° C and after one hour, it was quickly cooled in a mixture of ice and water. The samples were subjected to a tensile test and the results are summarized below.
In the ferrite sample, the amplitude was approximately between 30-40 dB, which is related to the deformation of the ferrite, while the amplitude in the martensite sample was between 40-45 dB, which

is related to the fracture of martensite. The maximum rise time in the ferrite sample was about 700-800 microseconds, while the maximum rise time in the martensite sample reached 2400 microseconds. The FFT method was used to take the dominant frequency and the outcomes illustrated that the ferrite phase deformation has a frequency of about 175 kHz, while this frequency range for the martensite phase was about 520-700 kHz.

In the ferrite sample, the SF had an ascending state after yielding. This indicates that the ratio of the AE energy released during the tensile test was lower than the strain energy, while the SF in the martensite sample was almost constant until before 0.004 strain and indicates a relative balance between AE energy and strain energy. After this strain, the SF takes a downward state and indicates a greater ratio of acoustic energy to strain energy.

To better identify the behavior of dual-phase steels, it is necessary to investigate the ferrite and martensite phases. The results obtained in this research show that the use of the AE method and signal analysis by the SF method is so effective. By using this method, the behavior of dual-phase steels with different percentages of martensite phase in the structure can be investigated in other research.

## 6. References

[1] Afsari, A., Fazel, D., Karimisharifabadi, J. and Mehrabi, V. 2020. Study the Percentage of Carbon and Ferrite in Layers of Steel (SA-516) by Strip Cladding with E316L. Journal of Modern Processes in Manufacturing and Production. 9(3): 41-50.

[2] Salari, M. 2019. Texture Evolution in Low Carbon Steel Fabricated by Multi-directional Forging of the Martensite Starting Structure. Journal of Modern Processes in Manufacturing and Production. 8(4): 5-15.

[3] Verhoeven, J. D. 2005. Metallurgy of steel for bladesmiths & others who heat treat and forge steel. Iowa State University. Ph.D. Thesis.

[4] Maki, T. 2012. Morphology and substructure of martensite in steels. Phase Transformations in Steels. Elesevier.

[5] Vahaviolos, S. J. 1999. Acoustic Emission: Standards and Technology Update (Vol. 1353). ASTM International.

[6] Khamedi, R., Fallahi, A. and Oskouei, A. R. 2010. Effect of martensite phase volume fraction on acoustic emission signals using wavelet packet analysis during tensile loading of dual phase steels. Materials & Design. 31(6): 2752-2759.

[7] Fallahi, A., Khamedi, R., Minak, G. and Zucchelli, A. 2012. Monitoring of the deformation and fracture process of dual phase steels employing acoustic emission techniques. Materials Science and Engineering. 548: 183-188.

[8] Van Bohemen, S. M. C., Sietsma, J., Hermans, M. J. M. and Richardson, I. M. 2003. Kinetics of the martensitic transformation in low-alloy steel studied by means of acoustic emission. Acta Materialia. 51(14): 4183-4196.

[9] Khamedi, R., Fallahi, A. and Zoghi, H. 2009. The influence of morphology and volume fraction of martensite on AE signals during tensile loading of dual-phase steels. International Journal of Recent Trends in Engineering. 1(5): 30-34.

[10] Khamedi, R., Fallahi, A., Refahi Oskouei, A. and Ahmadi, M. 2008. The effect of martensite phase volume fraction of dual-phase steels on acoustic emission signals under tensile loading. In 17th National Symposium on Ultrasonics Conference, Varanasi, India.

[11] Speich, G. R. and Schwoeble, A. J. 1975. Acoustic emission during phase. ASTM International. 571: 40-50.

[12] Rad, V. F., Khamedi, R. and Moradi, A. R. 2019. The effect of martensite volume fraction on topography of dual phase steels. Materials Letters. 239: 21-23.

[13] Kamel, S. M., Samy, N. M., Tóth, L. Z., Daróczi, L. and Beke, D. L. 2022. Denouement of the Energy-Amplitude and Size-Amplitude Enigma for Acoustic-Emission Investigations of Materials. Materials. 15(13): 4556.

[14] Ramalho, A., Santos, T. G., Bevans, B., Smoqi, Z., Rao, P. and Oliveira, J. P. 2022. Effect of contaminations on the acoustic emissions during wire and arc additive manufacturing of 316L stainless steel. Additive Manufacturing. 51: 102585.

[15] Speich, G. R. and Fisher, R. M. 1972. Acoustic emission during martensite formation. ASTM STP. 505: 140-151.

[16] Planes, A., Mañosa, L. and Vives, E. 2013. Acoustic emission in martensitic transformations. Journal of Alloys and Compounds. 577: 699-704.

[17] Khosravi, M. and Khamedi, R. 2022. Investigation of the effect of ferrite grain size on acoustic emission signals. Journal of Modern Processes in Manufacturing and Production. 11(3): 61-68.

[18] Bayram, A., Uğuz, A. and Ula, M. 1999. Effects of microstructure and notches on the mechanical properties of dual-phase steels. Materials characterization. 43(4): 259-269.

[19] Dieter, P. P. 1988. Mechanical Metallurgy. McGraw-Hill Book. New York 1986.

[20] JH, H. and DM, L. 1999. Acoustic emission behavior during tensile tests of low carbon steel welds. ISIJ International. 39(4): 365-370.

[21] Huh, J. H., Lee, K. A. and Lee, C. S. 1997. Acoustic emission behavior during tensile deformation of welded steel joints. International Nuclear Information System. 45(29): 80-88.

[22] Raj, B., Jha, B. B. and Rodriguez, P. 1989. Frequency spectrum analysis of acoustic emission signal obtained during tensile deformation and fracture of an AISI 316 type stainless steel. Acta metallurgical. 37(8): 2211-2215.

[23] Casey, N. F., White, H. and Taylor, J. L. 1985. Frequency analysis of the signals generated by the failure of constituent wires of wire rope. NDT international. 18(6): 339-344.